polymers

MDPI

Article

Micellization Studies of Block Copolymers of Poly(N-vinyl pyrrolidone) and n-Alkyl-Substituted Poly(vinyl esters) in Tetrahydrofuran

Nikoletta Roka *, Vasileios-Christos Skiadas, Areti Kolovou, Theodosia-Panagiota Papazoglou and Marinos Pitsikalis

Industrial Chemistry Laboratory, Department of Chemistry, National and Kapodistrian University of Athens, Panepistimiopolis Zografou, 15771 Athens, Greece; bill.skd@hotmail.com (V.-C.S.); aretikolovou.chem@gmail.com (A.K.); pnpapazoglou@gmail.com (T.-P.P.); pitsikalis@chem.uoa.gr (M.P.)
* Correspondence: nikolettaroka@yahoo.gr

Abstract

The association behavior of amphiphilic block copolymers of N-vinyl pyrrolidone (NVP) and several vinyl esters (Ves) (PNVP-b-PVEs), as exemplified by vinyl butyrate (VBu), vinyl decanoate (VDc), and vinyl stearate (VSt), was studied in tetrahydrofuran (THF), which serves as the selective solvent for the PVE blocks. Static (SLS) and dynamic light scattering (DLS) techniques were adopted as the tools to investigate micellar properties and acquire information regarding the degree of association, the hydrodynamic radii, and the shape of the aggregates. In addition, CONTIN analysis provided insights concerning the association equilibria in THF solutions. The effect of the chemical structure of the corona-forming PVE block on the association process was investigated. Finally, the experimental results were compared with those obtained in previous studies describing the micellization properties of block copolymers consisting of PNVP and polymethacrylate blocks in the same selective solvent.

Keywords: poly(N-vinyl pyrrolidone) (NVP); poly(vinyl esters) (VEs); amphiphilic block copolymers; micelles; light scattering

check for updates

Academic Editor: Leonard Ionut Atanase

Received: 2 October 2025
Revised: 15 October 2025
Accepted: 22 October 2025
Published: 24 October 2025

Citation: Roka, N.; Skiadas, V.-C.; Kolovou, A.; Papazoglou, T.-P.; Pitsikalis, M. Micellization Studies of Block Copolymers of Poly(N-vinyl pyrrolidone) and n-Alkyl-Substituted Poly(vinyl esters) in Tetrahydrofuran. *Polymers* **2025**, *17*, 2842. https://doi.org/10.3390/polym17212842

Copyright: © 2025 by the authors. Licensee MDPI, Basel, Switzerland. This article is an open access article distributed under the terms and conditions of the Creative Commons Attribution (CC BY) license (https://creativecommons.org/licenses/by/4.0/).

1. Introduction

The most fascinating class of polymeric materials is without any doubt the family of block copolymers [1,2]. This is attributed to the following main reasons: (a) Block copolymers consist of two or more distinct polymer segments covalently linked in a linear sequence. This unique structure allows them to exhibit diverse characteristics, which are contingent upon the specific polymers used and their arrangement [3–5]. (b) There are numerous combinations of different blocks that can be combined in one structure, such as hydrophilic, hydrophobic, amorphous, crystalline, flexible, rigid materials, etc. [6,7]. (c) Well-defined copolymers with narrow molecular weight distributions and low chemical heterogeneity can be synthesized through a huge variety of polymerization techniques and combinations such as anionic, cationic, controlled radical, ring opening, ring opening metathesis, and coordination polymerization [8–24]. (d) Block copolymers employ their unique characteristic to promote self-assembly. This means that they are organized as supramolecular structures either in the absence of any solvent or in solvents good for one of the blocks [25,26]. In the absence of any solvent, the self-organization process produces specific microstructures, such as cylindrical, spherical, lamellar and cubic microphases,

etc. [27,28], whereas in solvents selective for one of the blocks to the formation of micellar structures [29–33], the micelles usually adopt the core–corona structure [34–36]. The non-soluble block forms the core, whereas the surrounding protective soluble block forms the corona of the supramolecular assemblies.

Amphiphilic block copolymers are a special subclass of copolymers bearing one block that is water-soluble and another one that is insoluble in water [37–43]. The characteristic of these structures is that they offer the possibility to self-assemble both in water and in suitable organic solvents. For this reason, countless applications have appeared in the literature based on these materials, including the fields of drug encapsulation and delivery, the biomedical sector (nanocarriers for gene therapy, stimuli-responsive drug carriers, biodegradable hydrogels, etc.), coating and surface modification (antifouling coatings, self-healing applications, etc.), nanotechnology and electronics (nanoreactors, nanocatalysis, organic electronics, flexible displays, etc.), cosmetics and personal care products (surfactants, emulsifiers, encapsulation of active ingredients, etc.), and water purification systems, etc., [39,44–53].

In previous studies, the preparation of various amphiphilic statistical and block copolymers has been reported based on poly(N-vinyl pyrrolidone) (PNVP) as the hydrophilic block and several polymethacrylates and poly(vinyl ethers) (PVEths) as the water-insoluble blocks, and their micellization behavior was examined both in specific organic solvents and in water [5,54–62]. In the frame of this project, diblock copolymers consisting of PNVP and poly(vinyl esters) (PVEs) with alkyl side groups were synthesized and thoroughly characterized [63]. More specifically, the synthesis of block copolymers (PNVP-b-PVEs) with poly(vinyl butyrate) (PVBu) poly(vinyl decanoate) (PVDc), and poly(vinyl stearate) (PVSt) blocks was reported by employing Reversible Addition Fragmentation Chain Transfer (RAFT) approaches.

Previous efforts have been documented for the preparation of statistical and block copolymers of various PVEs. Most of them were based on poly(vinyl acetate), PVAc [64–66]. However, other VE monomers have been employed as well, including vinyl pivalate, vinyl benzoate, and vinyl octanoate [67–71]. The most frequently mentioned system in the literature is that of PNVP-b-PVAc block copolymers. The main target of these works was the study of the micellar properties of these copolymers in aqueous solutions and their ability to encapsulate hydrophobic compounds and perform as potential drug delivery systems. On the other hand, only a few works describing the synthesis of diblocks between NVP and other VEs have been previously published in the literature, and in addition no effort was given to provide results regarding the micellization properties of these diblocks in organic solvents that are good solvents exclusively for the PVE blocks.

In order to fill this gap in the literature, the self-assembly behavior of PNVP-b-PVBu, PNVP-b-PVDc, and PNVP-b-PVSt was studied in tetrahydrofuran (THF), which is a selective solvent for the PVE blocks and a non-solvent for the PNVP blocks [72].

2. Materials and Methods

The values of the refractive index increments, dn/dc, at 25 °C were determined using a Chromatix KMX-16 refractometer (Milton Roy, LDC Division, Riviera Beach, FL, USA), which operates at 633 nm and was calibrated with solutions of sodium chloride in water.

Dynamic light scattering, DLS, experiments were carried out on a BI-200SM goniometer system (Brookhaven Instruments, Holtsville, NY, USA), which is equipped with a 40 mW laser at a wavelength of 640 nm. Correlation functions were analyzed using both the cumulant method and the CONTIN software package (Brookhaven Instruments, Holtsville, NY, USA) [73]. Data were collected at scattering angles of 45°, 90°, and 135° at a temperature

of 25 °C. For DLS measurements, five replicates were performed for each concentration, whereas every sample was measured twice, starting from different initial concentrations.

In all micellar systems studied, the angular dependence of the Γ/q^2 ratio (Γ denotes the correlation function's decay rate, and q denotes the scattering vector) was negligible. Therefore, the values of the apparent translational diffusion coefficients at infinite dilution, $D_{o,app}$, were extracted using Equation (1):

$$D_{app} = D_{0,\,app}(1 + kDc) \quad (1)$$

The corresponding apparent hydrodynamic radii, R_h, were calculated by employing the relation of Stokes–Einstein (Equation (2)):

$$R_h = kT/6\pi\eta_s D_{0,\,app} \quad (2)$$

with k being the Boltzmann's constant and T being the absolute temperature, whereas η_s is the solvent viscosity.

Static light scattering, SLS, experiments were conducted using the same BI-200SM system used for the DLS measurements, and data were processed using the Zimm plot module of the Particle Explorer software (v1.2.0.6868, Brookhaven Instruments, Holtsville, NY, USA). The data was collected at 25 °C at the scattering angles of 45°, 60°, 75°, 90°, 105°, 120°, and 135°. SLS measurements were conducted in ten replicates for each concentration. Again, every sample was measured twice, starting from different initial concentrations.

For all the measurements, initially a stock solution was prepared by direct dissolution of the respective sample in THF. The solvent was previously dried overnight in sodium and distilled just prior to its employment. The stock solutions were left overnight at room temperature, and then gently heated in an oven at 40 °C for at least 3 h, thus facilitating the dissolution of the polymers and obtaining micellar structures in equilibrium. The stock solutions were further diluted with dry THF to obtain lower-concentration solutions. The range of concentrations for all the samples was between 5×10^{-3} and up to 7×10^{-2} g/mL for both SLS and DLS measurements. Although all samples appeared crystal-clear without turbidity or insoluble particles, they were filtered through 0.22 μm pore size hydrophobic PTFE filters (Millex-LCR, Millipore, Cork, Ireland) to ensure the removal of any dust before being directly introduced into the scattering cell in the order of increasing concentration.

Viscometry measurements of dilute solutions were conducted at 25 °C using Cannon-Ubbelohde dilution viscometers (State College, PA, USA) with a Scott-Geräte AVS 410 automatic flow timer (Heidelberg, Germany). Viscometric data were analyzed by employing both the Huggins equation

$$\eta_{sp}/c = [\eta] + k_H[\eta]^2 c + \ldots \quad (3)$$

and the Kraemer equation

$$\ln\eta_r/c = [\eta] + k_K[\eta]^2 c + \ldots \quad (4)$$

where η_r, η_{sp}, and $[\eta]$ are the relative, specific, and intrinsic viscosities, respectively. Moreover, k_H and k_K are the Huggins and Kraemer constants, respectively. Viscometric radii, R_v, were calculated from the equation

$$R_v = (3/10\pi N_A)^{1/3}([\eta]\, M_{w,app})^{1/3} \quad (5)$$

where $M_{w,app}$ is the average molecular weight determined by light scattering measurements.

Transmission electron microscopy (TEM) experiments were carried out using a Hitachi HT7800. Carbon-coated copper TEM grids with a size of 200 mesh (ProSciTech Pty. Ltd., Thuringowa, Australia) were employed. An aliquot (5 μL) of the sample was pipetted

onto each grid. The solution was allowed to be adsorbed for 1 min. The grids were then manually blotted using Whatman 541 filter paper to remove the excess liquid on the grids. The grids were then left to air-dry at room temperature for approximately 10 min. No staining protocol was applied to the grid preparation for all samples.

3. Results and Discussion

3.1. Preparation of the Block Copolymers of NVP and VEs

The synthesis of the PNVP-b-PVEs was described in detail in a previous publication [63]. Very briefly, the polymerization of NVP was initially carried out using O-ethyl S-(phthalimidylmethyl) xanthate, which served as the CTA. The produced polymer was isolated, purified, characterized, and further used as the macro-CTA for the subsequent polymerization of the respective VE monomer, enabling the formation of well-defined block copolymers. Table 1 summarizes the molecular characteristics of these blocks (average molecular weights, M_n, and dispersity values, Đ).

Table 1. Molecular features of the block copolymers.

	Macro CTA (PNVP) [a]		Block Copolymers [a]		NVP	Vinyl Ester
Sample	**M_n 10^3 (Daltons)**	**Đ**	**M_n 10^3 (Daltons)**	**Đ**	**% mol [b]**	**% mol [b]**
PNVP-b-PVBu #1	8.5	1.30	16.0	1.90	22	78
PNVP-b-PVBu #2	8.9	1.35	15.5	1.54	48	52
PNVP-b-PVBu #3	8.9	1.35	17.5	1.40	57	43
PNVP-b-PVBu #4	28.0	1.27	32.0	1.32	84	16
PNVP-b-PVDc #1	5.5	1.47	12.5	1.60	38	62
PNVP-b-PVDc #2	8.5	1.30	11.0	1.45	56	44
PNVP-b-PVDc #3	8.5	1.30	12.5	1.31	63	37
PNVP-b-PVDc #4	9.5	1.36	10.5	1.36	93	7
PNVP-b-PVSt #1	7.5	1.30	10.4	1.51	61	39
PNVP-b-PVSt #2	8.5	1.30	10.5	1.44	78	22
PNVP-b-PVSt #3	8.1	1.30	12.5	1.22	83	17
PNVP-b-PVSt #4	8.1	1.30	10.9	1.37	85	15

a. by SEC in $CHCl_3$. b. by ^{1}H-NMR.

3.2. Self-Assembly Behavior of the PNVP-b-PVE Block Copolymers in THF Solutions by Static Light Scattering

Table 2 lists the SLS data from the PNVP-b-PVEs block copolymers in THF, whereas characteristic Zimm graphs from these measurements are presented in Figures 1–3.

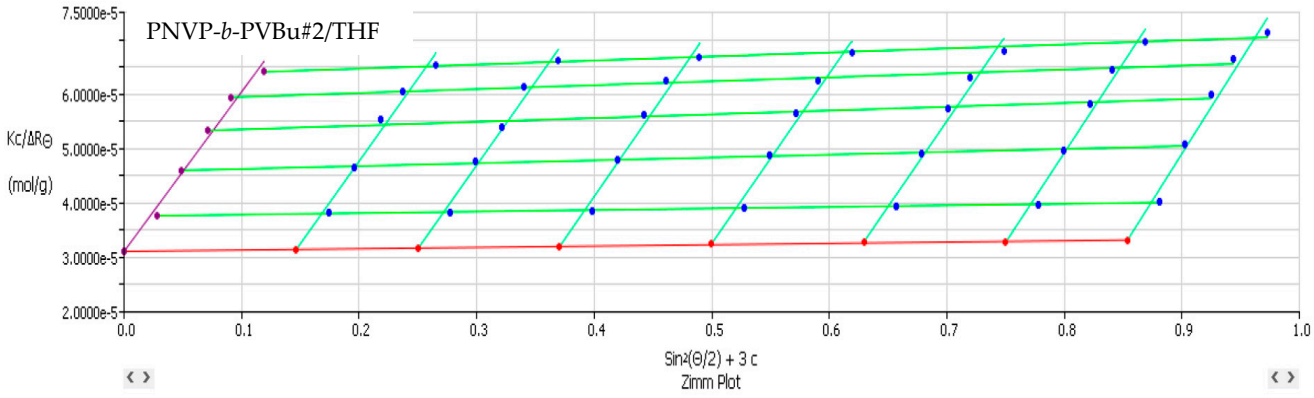


Figure 1. Zimm plot ($Kc/\Delta R_\theta$ vs. $\sin^2(\theta/2)$) corresponding to PNVP-b-PVBu #2 in THF.

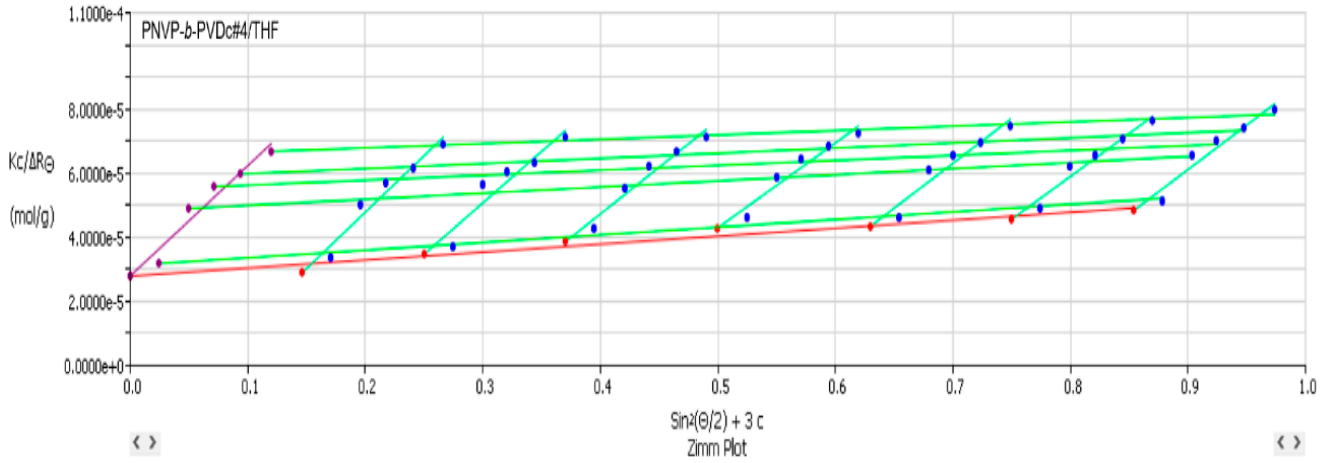


Figure 2. Zimm plot ($Kc/\Delta R_\theta$ vs. $\sin^2(\theta/2)$) corresponding to PNVP-b-PVDc #4 in THF.

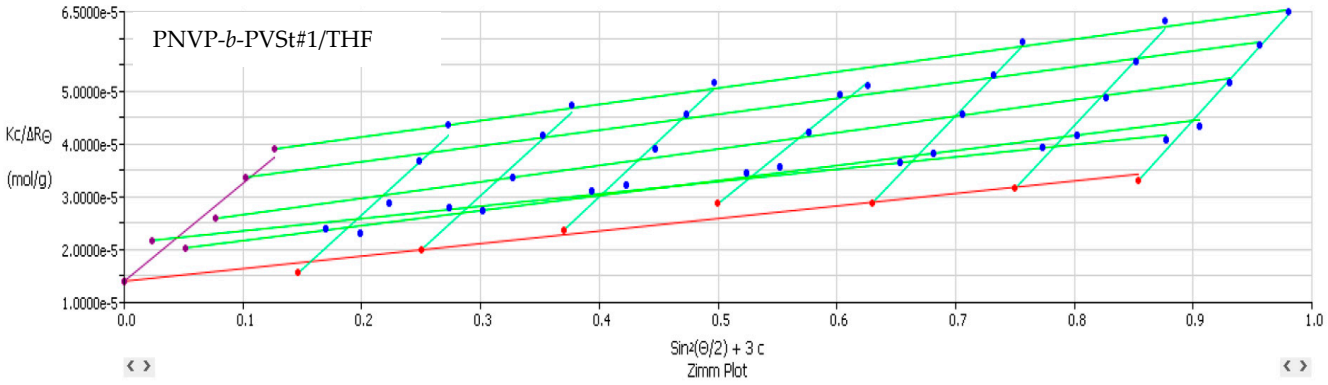


Figure 3. Zimm plot ($Kc/\Delta R_\theta$ vs. $\sin^2(\theta/2)$) corresponding to PNVP-b-PVSt #1 in THF.

Table 2. SLS results of PNVP-b-PVE block copolymers in THF.

Sample	$M_w \times 10^{-4}$	N_w	$A_2 \times 10^4$ (cm^3 mol/g^2)
PNVP-b-PVBu #1	15.9	9.94	1.40
PNVP-b-PVBu #2	3.22	2.08	4.39
PNVP-b-PVBu #3	3.62	2.07	3.86
PNVP-b-PVBu #4	5.69	1.78	0.69
PNVP-b-PVDc #1	6.35	5.08	2.07
PNVP-b-PVDc #2	3.35	3.05	2.50
PNVP-b-PVDc #3	10.5	8.40	3.50
PNVP-b-PVDc #4	3.59	3.42	5.16
PNVP-b-PVSt #1	7.13	6.86	2.78
PNVP-b-PVSt #2	3.82	3.64	1.48
PNVP-b-PVSt #3	18.6	14.88	1.90
PNVP-b-PVSt #4	4.44	4.07	1.30

It is of paramount importance to verify that the micellar solutions are in equilibrium when performing light scattering measurements. Heating the initial stock solution for several hours is usually enough to promote equilibrium structures, especially when the supramolecular structures are not very large, as seen in this case. Verification was made by employing measurements starting with stock solutions of different initial concentrations. If the solutions are not under equilibrium, the different stock solutions would provide different results regarding the degree of association and the hydrodynamic radius. In

our case all the results were comparable, confirming that the samples are in thermodynamic equilibrium.

In previous studies examining the self-assembly properties of statistical and block copolymers of PNVP with polymethacrylates, it was concluded that THF is not able to promote the formation of large multimolecular micelles [54,61]. The weight-average degrees of association, N_w, were higher in the case of the block copolymers [55]. Nevertheless, even in this case, the N_w values were not very high ($N_w < 10$). These results look reasonable for the statistical copolymers due to the specific distribution of the individual monomer units along the polymer backbone. However, for the block copolymers with two distinct constituent chains connected with a covalent bond, it would be expected that a more pronounced association behavior could be feasible. The main conclusion from the previous systems is that unimolecular micelles are primarily produced from statistical copolymers, in contrast to the block copolymers, which form compact micelles with a low aggregation number in THF solutions.

This behavior was more or less confirmed in the present study, which studies the self-organization process of the PNVP-b-PVE block copolymers in THF. The experimental data from the SLS measurements revealed low aggregation numbers in almost all cases. This can be attributed to the comparatively reduced molecular weights of the samples. However, the main reason is correlated with the low ability of THF to promote the formation of large aggregates. Slightly higher N_w values were measured for the PNV-b-PVSt copolymers, indicating that the long alkyl side chain of the corona-forming block, PVSt, through hydrophobic interactions, further stabilizes the corona of the supramolecular structures or even facilitates intermicellar interactions, leading to more complex patterns of association.

It has to be mentioned that the copolymers containing the greatest proportion of PNVP have slightly lower N_w values, meaning that compact crew-cut star-like micelles prevail in THF solutions. The surrounding corona of the supramolecular structures with the extended side alkyl chains of the respective PVEs is able to stabilize lower aggregation numbers. In addition, the reduced values of the second virial coefficient, A_2, from SLS measurements in THF solutions verify the existence of micelles with unimolecular characteristics or a low aggregation number. A similar behavior has been observed in the case of statistical and block copolymers of PNVP and polymethacrylates.

3.3. Self-Assembly Behavior of the PNVP-b-PVE Block Copolymers in THF Solutions by Dynamic Light Scattering

The findings obtained from SLS measurements were additionally validated and elucidated by the DLS results. CONTIN analysis is able to offer distribution analysis of the various populations that may be present in the selective solvent. Therefore, DLS data provide deeper insight into the micellization process. Table 3 summarizes the specific data, while characteristic DLS plots from the various copolymer families are shown in Figures 4–6.

As expected, the DLS measurements confirm and further fortify the corresponding SLS data. Regarding the PNVP-b-PVBu copolymer, CONTIN analysis revealed the presence of two distinct populations in the THF solutions. Characteristic CONTIN plots for sample PNVP-b-PVBu #3 are given in Figure 7. Judging from their relative size, it can be concluded that there is an equilibrium between unimolecular and typical core–shell multimolecular micelles. The unimolecular micelles dominate in the selective solvent, since the high-R_h-value population ranges between 25 and 50% in all concentrations and for all samples. Taking into account that larger particles provide higher scattering intensity values than the small ones, it can be derived that the contribution of the multimolecular micelles is much less than 20% in the solution. This finding aligns with the reduced degrees of association measured by SLS measurements.

Table 3. Summary of DLS measurements for block copolymers in THF.

Sample	Do (cm^2/s)	K_d	R_{ho} A (nm)	R_{ho} B (nm)
PNVP-b-PVBu #1	11.2405	2.04	4.22	48.45
PNVP-b-PVBu #2	10.4839	4.63	4.53	32.97
PNVP-b-PVBu #3	9.9667	8.58	4.76	170.06
PNVP-b-PVBu #4	9.19953	−2.98	5.16	96.31
PNVP-b-PVDc #1	14.2491	0.96	3.33	35.82
PNVP-b-PVDc #2	11.6172	5.81	4.08	76.10
PNVP-b-PVDc #3	15.1746	−1.11	3.13	15.58
PNVP-b-PVDc #4	14.0547	0.29	3.38	85.11
PNVP-b-PVSt #1	13.2195	1.37	3.59	81.37
PNVP-b-PVSt #2	12.2076	3.09	3.89	71.94
PNVP-b-PVSt #3	13.8421	1.40	3.43	94.93
PNVP-b-PVSt #4	14.3697	0.32	3.30	84.08

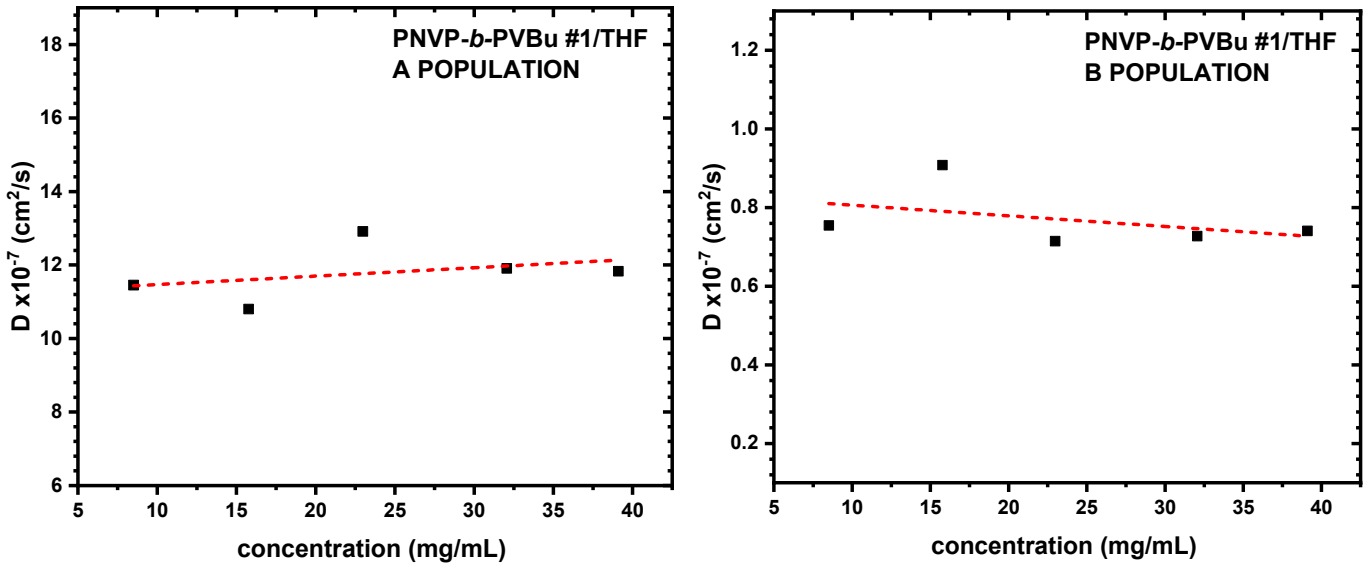


Figure 4. D vs. c plots of PNVP-b-PVBu #1 in THF.

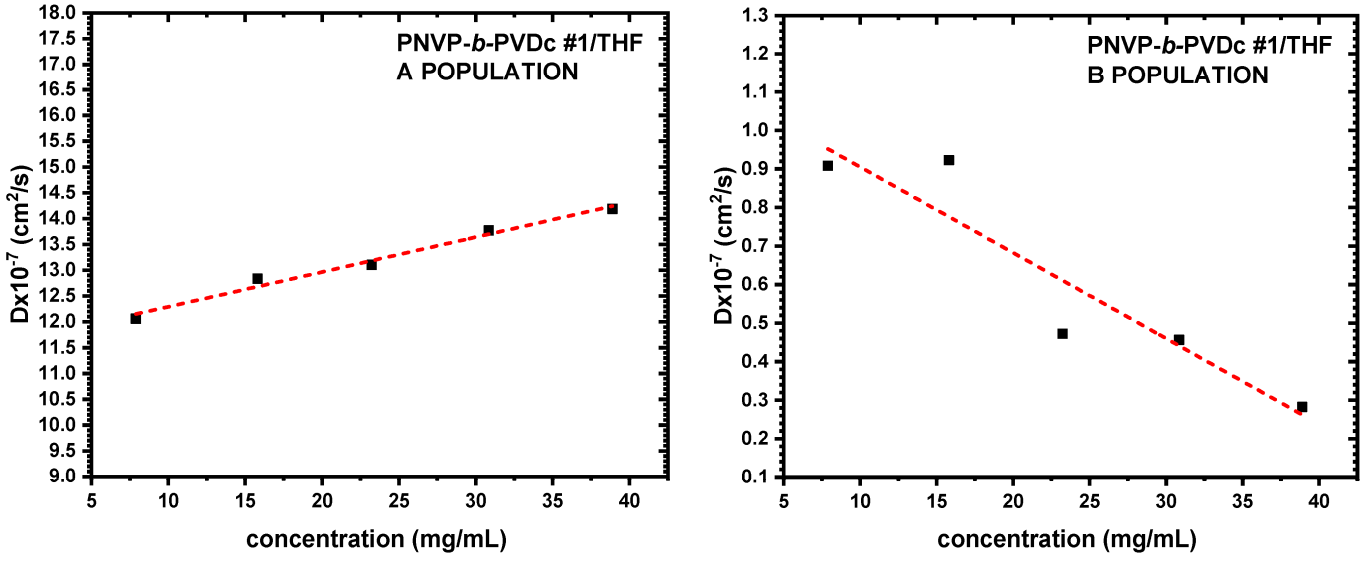


Figure 5. D vs. c plots of PNVP-b-PVDc #1 in THF.

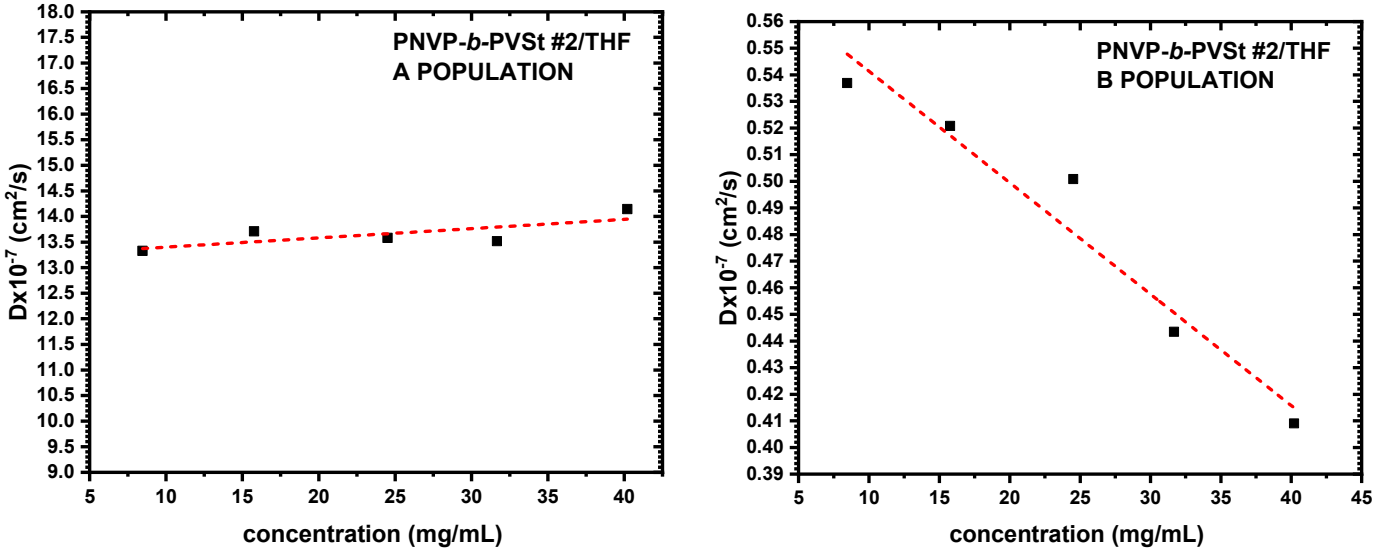


Figure 6. D vs. c plots of PNVP-b-PVSt #2 in THF.

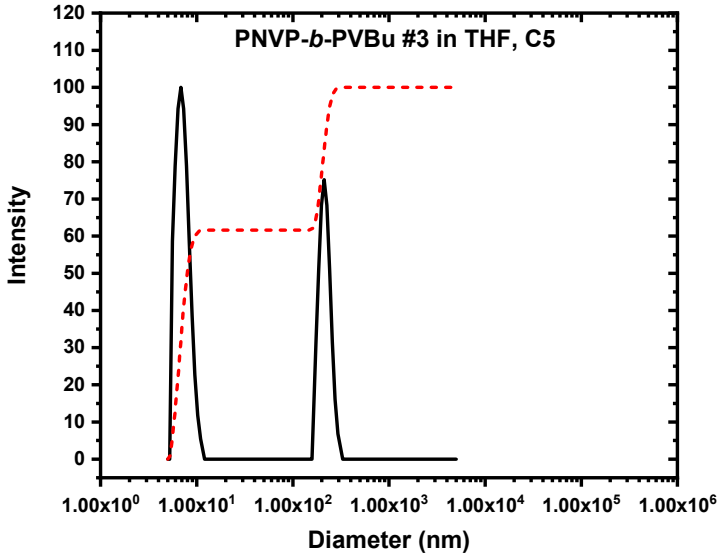


Figure 7. CONTIN plots (black line scattering intensity vs. diameter) of PNVP-b-PVBu #3 (c = 3.953 $\times$ 10^{-2} g/mL). The red line is the integration line of the two peaks.

The k_D levels in THF were low, as was expected from the modest A_2 values from the SLS data. This outcome is justifiable given the established relationship between k_D and A_2, which is defined by the equation below.

$$k_D = 2A_2M - k_f - u \quad (6)$$

In this equation M represents the molecular weight, k_f denotes the coefficient related to the concentration dependence of the friction coefficient, and u stands for the partial specific volume of the polymer.

In addition to these observations, no angular dependence was obtained from the DLS measurements, confirming the formation of spherical structures. Judging from the values of the polydispersity factor μ_2/Γ^2, with μ_2 being the second moment calculated via cumulant analysis and Γ being the correlation function's decay rate, these structures were relatively polydisperse. These values were higher than 0.1 for all samples.

The DLS results for PNVP-b-PVDc were comparable to those previously presented for the PNVP-b-PVBu samples. CONTIN plots verified the establishment of equilibrium between unimolecular and multimolecular micelles. An illustrative example is presented in Figure 8. The population of the core–shell micelles is in the same order as in the previous case (ranging between 20 and 50%); however, the R_h values of these structures are relatively lower compared to the multimolecular micelles coming from the PNVP-b-PVBu copolymers. This result indicates that the micelles with the corona from PVDc chains are more compact; this is attributable to the stronger hydrophobic interactions of the alkyl substituents of the PVDc chains. Otherwise, spherical, relatively polydisperse structures were obtained in this case as well.

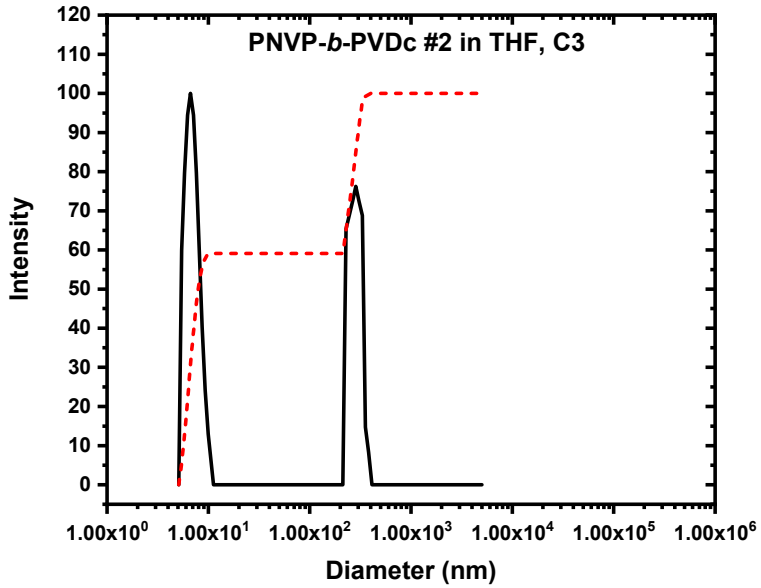


Figure 8. CONTIN plots (black line scattering intensity vs. diameter) of PNVP-b-PVDc #2 ($c = 2.436 \times 10^{-2}$ g/mL). The red line is the integration line of the two peaks.

The situation was slightly differentiated in regard to the PNVP-b-PVSt block copolymers. From the SLS data, it was concluded that the levels of association were relatively higher in comparison with the other two families of copolymers. The results from DLS and especially the CONTIN method demonstrated that the equilibrium is shifted in this case towards the micellar structures. Their population is typically more than 50% and up to 70% for specific copolymers and at higher concentrations. Of course, the real population, as explained earlier, is much lower; nevertheless, it is much higher than that of the other two types of block copolymers. The potential of stronger interactions among the PVSt chains, due to side chain crystallization, is responsible for this observation. Characteristic CONTIN plots are given in Figure 9. The second population is not only more pronounced in the overall content in the solution but also has considerably higher R_h values. Furthermore, the size of the second population is more uniform compared to the other two families of copolymers, indicating a similar process of organization. This is attributed to the high VSt content and the stronger hydrophobic interactions between the poly(vinyl ester) chains, which stabilize the multimolecular structures. Very low or even negative k_d values were measured across all cases, in accordance with the corresponding reduced A_2 values reported in the SLS measurements and the more extended association phenomena reported for this copolymerization system.

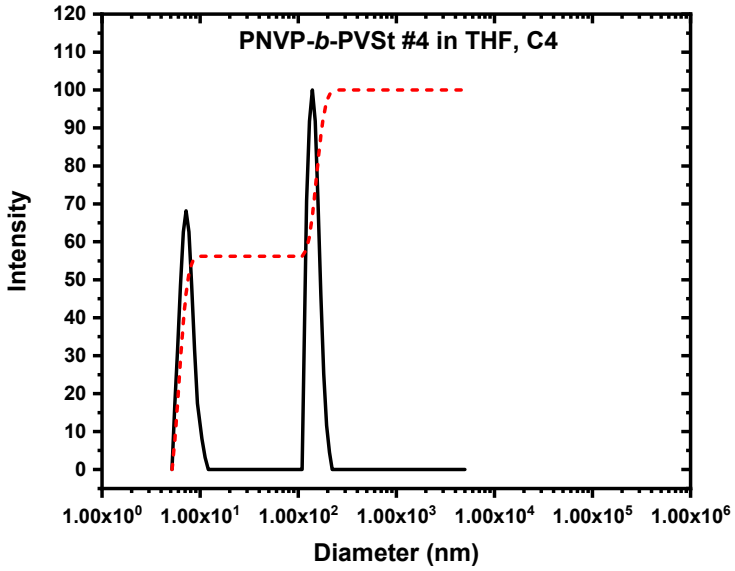


Figure 9. CONTIN plots (black line scattering intensity vs. diameter) of PNVP-b-PVSt #4 (c = 3.184 × 10^{-2} g/mL). The red line is the integration line of the two peaks.

Evaluating the self-assembly behavior in relation to other statistical and block copolymers of PNVP with polymethacrylates in the same selective solvent (THF) revealed similarities and differences. The degrees of associations are higher than those of the statistical copolymers, where unimolecular micelles almost exclusively dominate. However, compared to the respective block copolymers, the association behavior is more pronounced, especially with respect to the PNVP-b-PVSt copolymers, where a higher tendency for the formation of multimolecular micelles was obtained. The polymethacrylates, as solvophilic blocks, generate small and compact micellar structures, as revealed by CONTIN plots without equilibrium and with unimolecular micelles. Therefore, the nature of the solvophilic block dramatically affects the self-assembly process.

3.4. Self-Assembly Behavior of the PNVP-b-PVE Block Copolymers in THF Solutions by Dilute Solution Viscometry

The viscometry data of the dilute solutions are given in Table 4, whereas characteristic plots from the measurements are shown in Figure 10.

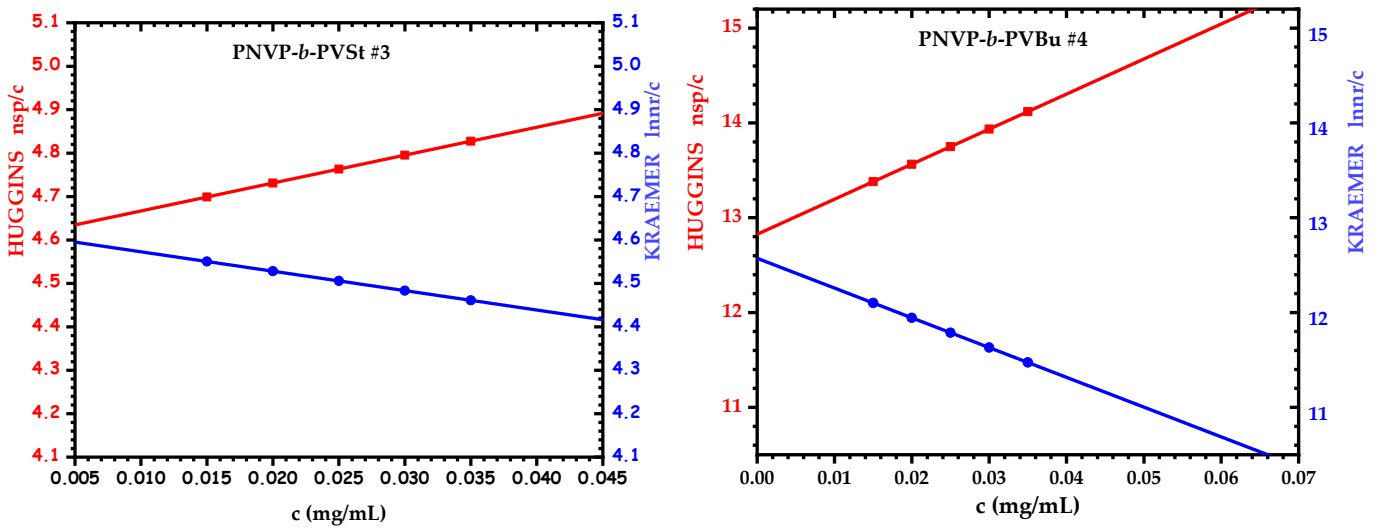


Figure 10. Viscometry plots of the dilute solutions for samples PNVP-b-PVBu#4 and PNVP-b-PVSt#3.

Table 4. Viscometry results of the dilute solutions in THF.

Sample	$[\eta]_H$ mL/g	$[\eta]_K$ mL/g	K_H	R_v, nm
PNVP-b-PVBu #1	12.30	11.92	0.33	6.76
PNVP-b-PVBu #4	12.82	12.57	0.43	4.87
PNVP-b-PVDc #1	8.22	7.84	0.36	4.36
PNVP-b-PVDc #2	5.64	5.64	0.41	3.10
PNVP-b-PVDc #3	6.56	6.30	0.59	4.78
PNVP-b-PVDc #4	5.01	5.17	1.07	3.05
PNVP-b-PVSt #1	3.51	3.52	0.59	3.41
PNVP-b-PVSt #2	1.97	2.11	1.60	2.82
PNVP-b-PVSt #3	4.60	4.62	0.30	5.14
PNVP-b-PVSt #4	8.00	7.46	1.20	3.83

The intrinsic viscosity values from both the Huggins and Kraemer approaches were in close agreement for all samples, confirming the validity of the methods. The K_H values were relatively high in most cases, although the intrinsic viscosity values were not very high. This result is a manifestation of the presence of strong hydrodynamic interactions in the THF solution, which occur as a result of the aggregation process. The R_v values are very close to the R_h values, as measured by DLS measurements corresponding to the first population in THF solutions. An equilibrium between unimolecular and multimolecular micelles is established according to the CONTIN analysis of the DLS data. The viscometry results of the dilute solutions confirm that the multimolecular micelles are not very stable and that they disassociate to the corresponding unimolecular micelles upon the existence of shear forces, which are developed in the capillary viscometer. This behavior has been previously reported in aggregating systems [74,75].

3.5. Self-Assembly Behavior of the PNVP-b-PVE Block Copolymers in THF Solutions by TEM Imaging

TEM images were collected on carbon-coated copper grids without performing staining. In an effort to enhance the contrast of the micellar structures and improve the quality of the TEM images, the grids were stained with uranyl acetate. However, this procedure was not efficient, since the strong interaction of the pyrrolidone rings with uranium resulted in a black surface without any possibility to identify supramolecular structures on the grids. Therefore, the images were obtained without staining. Characteristic images from the micellar solutions in THF are given in Figures 11–16.

These figures confirm the results that have been drawn from the DLS measurements. It is obvious that there is an equilibrium between large multimolecular micellar structures and very small unimolecular micelles. The large structures are polydisperse and seem to be constructed as assemblies of monomolecular micelles. This conclusion can explain how easily these structures disassemble to unimolecular micelles upon the application of shear forces during the flow of the solutions with the supramolecular structures in the capillary tube of the viscometer. Finally, the radii of the observed micellar entities from the TEM images seem to be larger than those measured by DLS. This result is reasonable and commonly observed in the literature, since in TEM imaging, the structures are expanded on the surface of the grid in the absence of any solvent [76,77].

This work will be further expanded with further analysis of the micellar characteristics of these block copolymers in aqueous solutions.

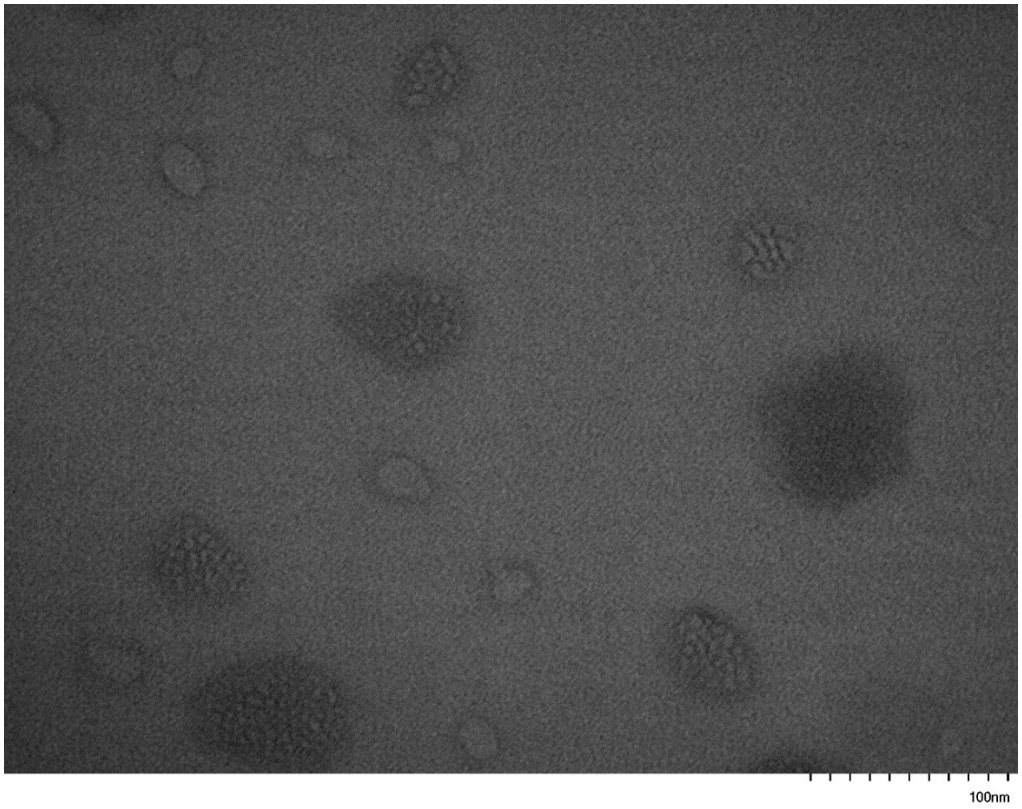


Figure 11. TEM image from sample PNVP-b-PVBu #3.

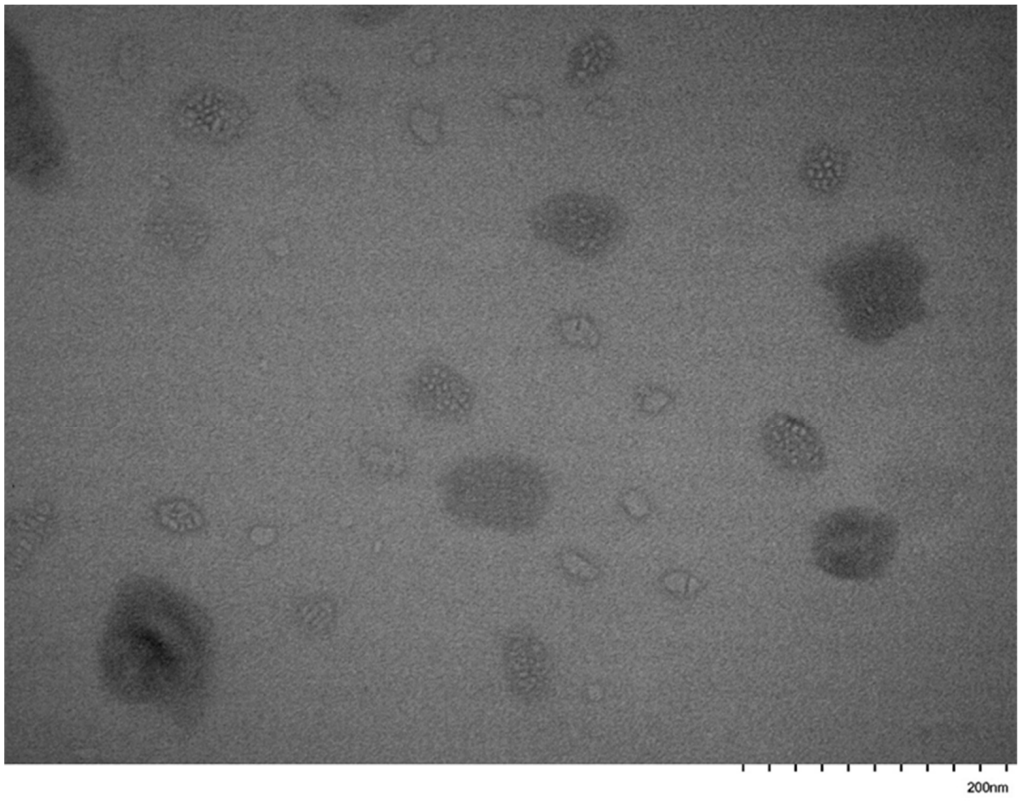


Figure 12. TEM image from sample PNVP-b-PVBu #2.

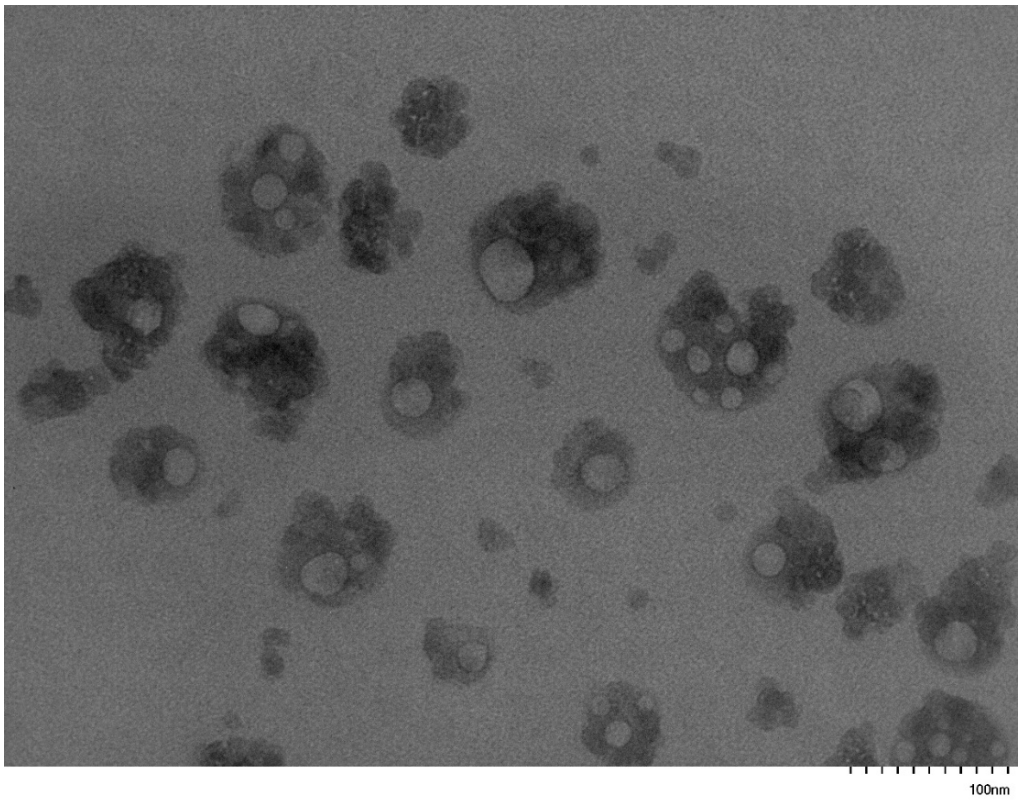


Figure 13. TEM image from sample PNVP-b-PVDc #2.

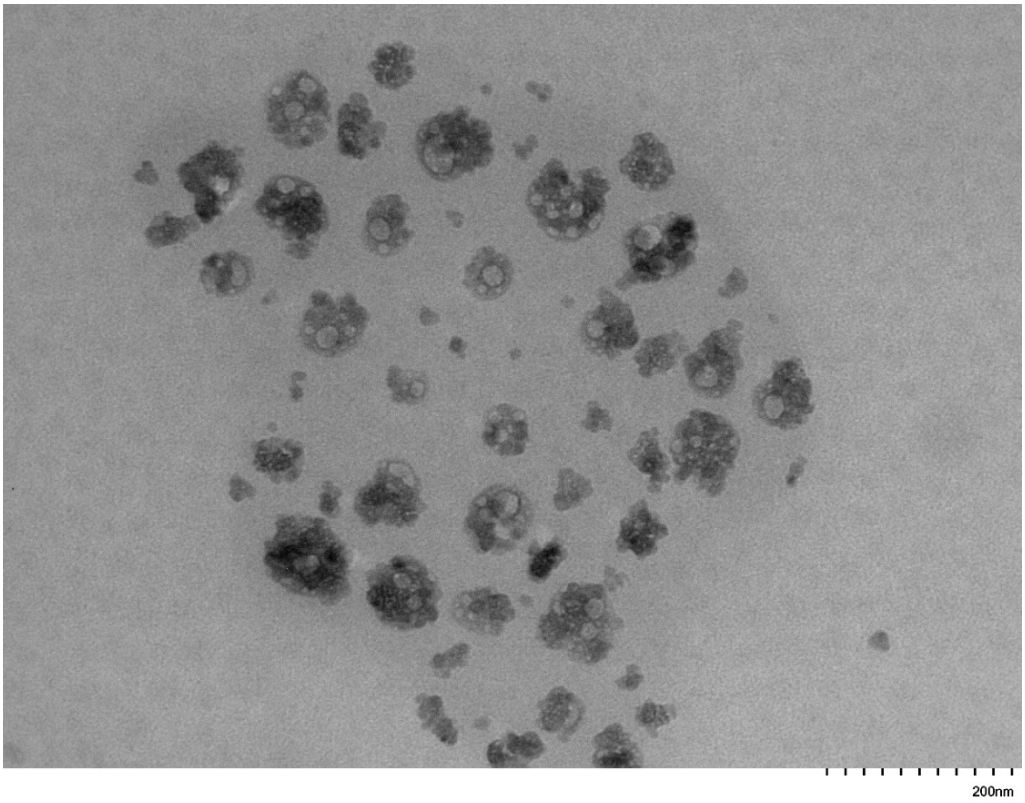


Figure 14. TEM image from sample PNVP-b-PVDc #4.

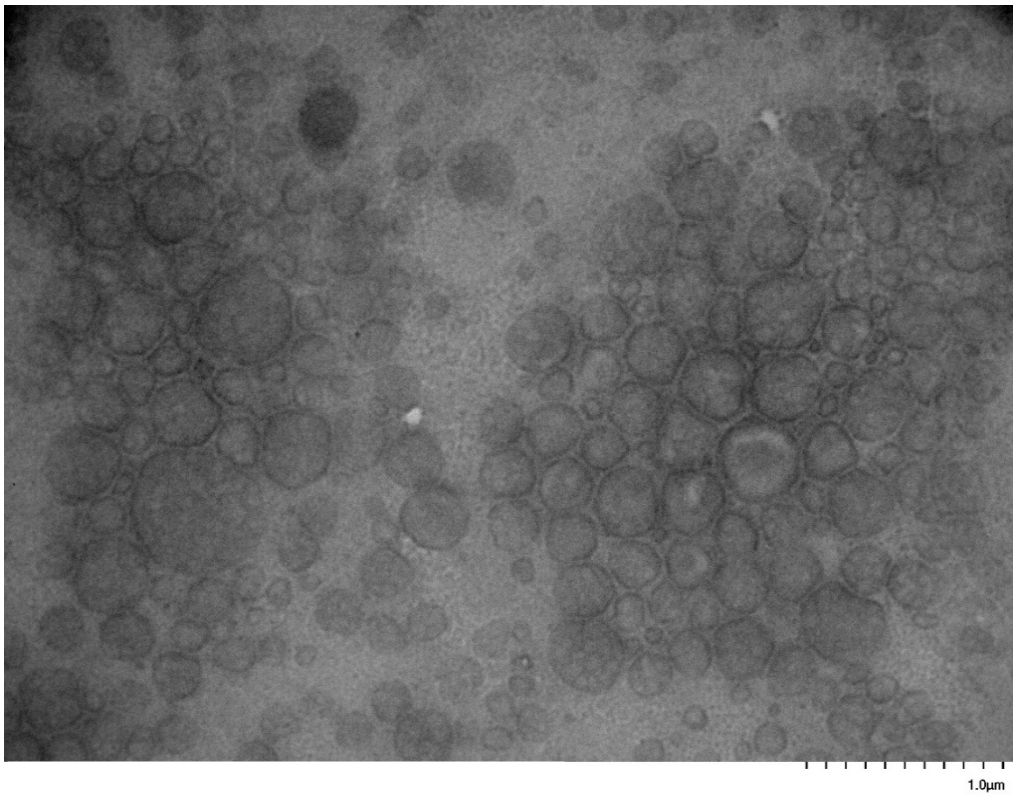


Figure 15. TEM image from sample PNVP-b-PVSt #1.

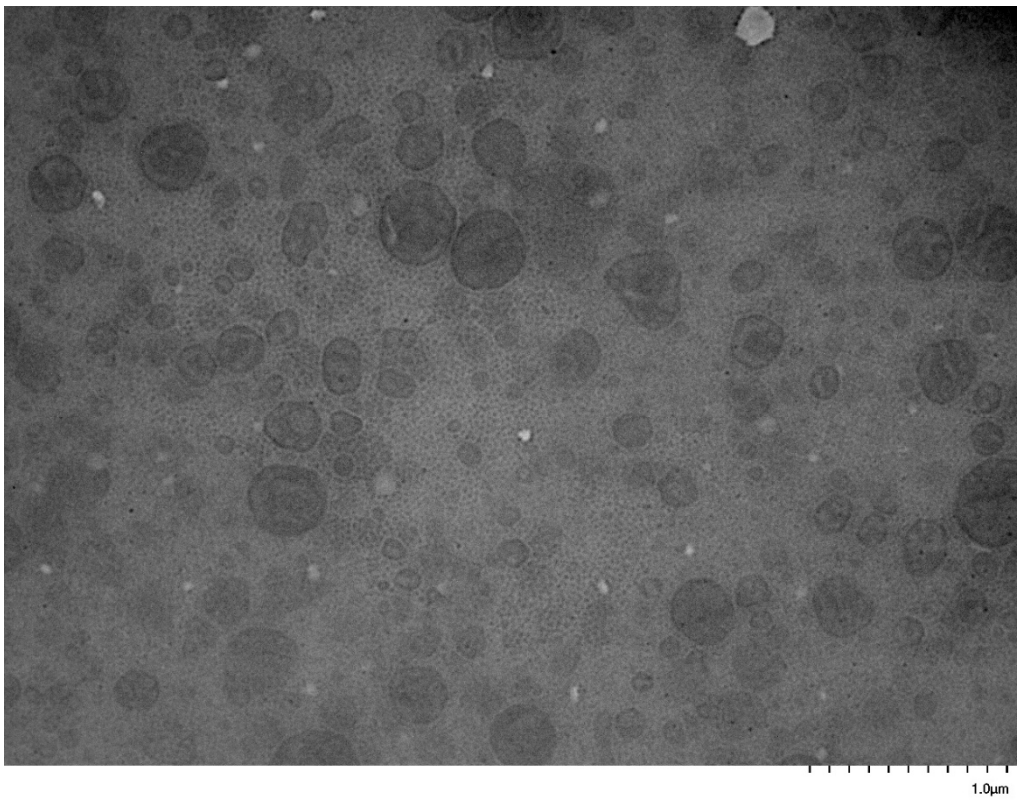


Figure 16. TEM image from sample PNVP-b-PVSt #2.

4. Conclusions

The self-assembly properties of amphiphilic block copolymers bearing a hydrophilic poly(N-vinyl pyrrolidone) (PNVP) block and several hydrophobic poly(vinyl ester), (PVE) blocks (PNVP-b-PVEs), including poly(vinyl butyrate) (PVBu), poly(vinyl decanoate) (PVDc), and poly(vinyl stearate) (PVSt), were explored in tetrahydrofuran (THF), which is a selective solvent for the PVE blocks. The studies were based on static (SLS) and dynamic light scattering (DLS) measurements. Rather low degrees of aggregation were found by SLS data, indicating the presence of unimolecular or small micelles in THF. More details concerning the association equilibria in THF solutions were traced by the DLS techniques and the CONTIN analysis. In all cases, an equilibrium between unimolecular and compact and spherical multimolecular micelles is established in THF solutions. Upon increasing the size of the alkyl side group of the PVE blocks, the equilibrium is shifted towards the multimolecular structures. In all cases the supramolecular structures are relatively polydisperse. These experimental results are in agreement with previous studies reporting the micellization properties of block copolymers of PNVP with polymethacrylates in the same selective solvent. However, in the present system, the trend towards the formation of multimolecular micelles is more pronounced, as revealed by the CONTIN analysis. These conclusions were further conformed by dilute solution viscometry measurements and TEM images.

Author Contributions: Conceptualization, M.P.; investigation, N.R., V.-C.S., A.K., and T.-P.P.; methodology, N.R.; supervision, M.P.; validation, M.P.; visualization, N.R.; writing—original draft, N.R.; writing—review and editing, M.P. All authors have read and agreed to the published version of the manuscript.

Funding: This research was co-financed by Greece and the European Union (European Social Fund-ESF) through the Operational Program «Human Resources Development, Education and Lifelong Learning» in the context of the project "Strengthening Human Resources Research Potential via Doctorate Research" (MIS-5000432), which was implemented by the State Scholarships Foundation (ΙΚΥ).

Data Availability Statement: The original contributions presented in this study are included in the article. Further inquiries can be directed to the corresponding author.

Acknowledgments: This research is co-financed by Greece and the European Union (European Social Fund- ESF) through the Operational Program «Human Resources Development, Education and Lifelong Learning» in the context of the project "Strengthening Human Resources Research Potential via Doctorate Research" (MIS-5000432), which was implemented by the State Scholarships Foundation (ΙΚΥ).

Conflicts of Interest: The authors declare no conflicts of interest.

References

1. Hadjichristidis, N.; Pispas, S.; Floudas, G.A. Block copolymers. In *Synthetic Strategies, Physical Properties and Applications*; John Wiley & Sons: Hoboken, NJ, USA, 2003.
2. Hamley, I.W. *The Physics of Block Copolymers*; Oxford University Press: Oxford, UK, 1998.
3. Hamley, I.W. (Ed.) *Developments in Block Copolymer Science and Technology*; Wiley: Chichester, UK, 2004.
4. Hadjichristidis, N.; Hirao, A.; Tezuka, Y.; Du Prez, F. (Eds.) *Complex Macromolecular Architectures: Synthesis, Characterization and Self-Assembly*; John Wiley & Sons (Asia) Pte Ltd.: Singapore, 2011.
5. Roka, N.; Kokkorogianni, O.; Kontoes-Georgoudakis, P.; Choinopoulos, I.; Pitsikalis, M. Recent Advances in the Synthesis of Complex Macromolecular Architectures Based on Poly(N-vinyl pyrrolidone) and the RAFT Polymerization Technique. *Polymers* **2022**, *14*, 701. [CrossRef]
6. Hadjichristidis, N.; Pitsikalis, M.; Iatrou, H. Synthesis of block copolymers. *Adv. Polym. Sci.* **2005**, *189*, 11–24.
7. Theodosopoulos, G.; Pitsikalis, M. Block Copolymers: Recent Synthetic Routes and Developments. In *Anionic Polymerization: Principles, Practice, Strength, Consequences and Applications*; Hadjichristidis, N., Hirao, A., Tezuka, Y., Du Prez, F., Eds.; John Wiley & Sons (Asia) Pte Ltd.: Singapore, 2011.

8. Hadjichristidis, N.; Pitsikalis, M.; Pispas, S.; Iatrou, H. Polymers with complex architectures by living anionic polymerization. *Chem. Rev.* **2001**, *101*, 3747–3792. [CrossRef]
9. Hadjichristidis, N.; Hirao, A. (Eds.) *Anionic Polymerization: Principles, Practice, Strength, Consequences and Applications*; Springer: Tokyo, Japan; Heidelberg, Germany; New York, NY, USA; Dordrecht, The Netherlands; London, UK, 2015.
10. Kennedy, J.P. Living cationic polymerization of olefins. How did the discovery come about? *J. Polym. Sci. Part A Polym. Chem.* **1999**, *37*, 2285–2293. [CrossRef]
11. Webster, O.W. The discovery and commercialization of group transfer polymerization. *J. Polym. Sci. Part A Polym. Chem.* **2000**, *38*, 2855–2860. [CrossRef]
12. Leitgeb, A.; Wappel, J.; Slugovc, C. The ROMP toolbox upgraded. *Polymer* **2010**, *51*, 2927–2946. [CrossRef]
13. Matyjaszewski, K.; Davis, T.P. (Eds.) *Handbook of Radical Polymerization*; Wiley-Interscience: Hoboken, NJ, USA, 2002.
14. Martin, L.; Gody, G.; Perrier, S. Preparation of complex multiblock copolymers via aqueous RAFT polymerization at room temperature. *Polym. Chem.* **2015**, *6*, 4875–4886. [CrossRef]
15. Hadjichristidis, N.; Iatrou, H.; Pitsikalis, M.; Mays, J.W. Macromolecular architectures by living and controlled/living polymerizations. *Progr. Polym. Sci.* **2006**, *31*, 1068–1132.
16. Hadjichristidis, N.; Pitsikalis, M.; Iatrou, H.; Sakellariou, G. *Macromolecular Architectures by Living and Controlled/living Polymerizations in Controlled and Living Polymerizations. From Mechanisms to Applications*; Müller, A.H.E., Matyjaszewski, K., Eds.; Wiley VCH: Weinheim, Germany, 2009; pp. 343–443, Chapter 7.
17. Dau, H.; Jones, G.R.; Tsogtgerel, E.; Nguyen, D.; Keyes, A.; Liu, Y.-S.; Rauf, H.; Ordonez, E.; Puchelle, V.; Alhan, H.B.; et al. Linear block copolymer synthesis. *Chem. Rev.* **2022**, *122*, 14471–14553. [CrossRef] [PubMed]
18. Dey, A.; Hldar, U.; De, P. Block copolymer synthesis by the combination of living cationic polymerization and other polymerization methods. *Front. Chem.* **2021**, *9*, 644547. [CrossRef]
19. Diaz, C.; Mehrkhodavandi, P. Strategies for the synthesis of block copolymers with biodegradable polyester segments. *Polym. Chem.* **2021**, *12*, 783–806. [CrossRef]
20. Hatada, K.; Kitayama, T.; Vogl, O. (Eds.) *Macromolecular Design of Polymeric Materials*; Marcel Dekker Inc.: New York City, NY, USA, 1997; Chapters 3,4.
21. Matyjaszewski, K.; Xia, J. Atom transfer radical polymerization. *J. Chem. Rev.* **2001**, *101*, 2921–2990. [CrossRef]
22. Coessens, V.; Pintauer, T.; Matyjaszewski, K. Functional polymers by atom transfer radical polymerization. *Progr. Polym. Sci.* **2001**, *26*, 337–377. [CrossRef]
23. Hawker, C.J.; Bosman, A.W.; Harth, E. New polymer synthesis by nitroxide mediated living radical polymerizations. *Chem. Rev.* **2001**, *101*, 3661–3688. [CrossRef] [PubMed]
24. Buchmeiser, M.R. Homogeneous metathesis polymerization by well-defined group VI and group VIII transition-metal alkylidenes: Fundamentals and applications in the preparation of advanced materials. *Chem. Rev.* **2000**, *100*, 1565–1604. [CrossRef]
25. Khandpur, A.K.; Förster, S.; Bates, F.S.; Hamley, I.; Ryan, A.J.; Almdal, K.; Mortensen, K. Polyisoprene-polystyrene diblock copolymer phase diagram near the order-disorder transition. *Macromolecules* **1995**, *28*, 8796–8806. [CrossRef]
26. Floudas, G.; Vazaiou, B.; Schipper, F.; Ulrich, R.; Wiesner, U.; Iatrou, H.; Hadjichristidis, N. Poly(ethylene oxide-*b*-isoprene) diblock copolymer phase diagram. *Macromolecules* **2001**, *34*, 2947–2957. [CrossRef]
27. Abetz, V.; Simon, P.F.W. Phase behaviour and morphologies of block copolymers. *Adv. Polym. Sci.* **2005**, *189*, 125–212.
28. Bates, F.M.; Fredrickson, G.H. Block copolymer thermodynamics-theory and experiment. *Ann. Rev. Phys. Chem.* **1990**, *41*, 525–557. [CrossRef]
29. Webber, S.E.; Munk, P.; Tuzar, Z. (Eds.) *Solvents and Self-Organization of Polymers*; NATO ASI Series; Kluwer Academic Publishers: Dordrecht, The Netherlands, 1996; Volume 327.
30. Xie, H.Q.; Xie, D. Molecular design, synthesis and properties of block and graft copolymers containing polyoxyethylene segments. *Progr. Polym. Sci.* **1999**, *24*, 275–313. [CrossRef]
31. Gohy, J.-F. Block copolymer micelles. *Adv. Polym. Sci.* **2005**, *190*, 65–136.
32. Riess, G. Micellization of block copolymers. *Prog. Polym. Sci.* **2003**, *28*, 1107–1170. [CrossRef]
33. Rodrígeuz-Hernádez, J.; Chécot, F.; Gnanou, Y.; Lecommandoux, S. Toward 'smart' nano-objects by self-assembly of block copolymers in solution. *Prog. Polym. Sci.* **2005**, *30*, 691–724. [CrossRef]
34. Astafieva, I.; Zhong, X.F.; Eisenberg, A. Critical micellization phenomena in block polyelectrolyte solutions. *Macromolecules* **1993**, *26*, 7339–7352. [CrossRef]
35. Prochazka, K.; Bednar, B.; Mukhtar, E.; Svoboda, P.; Trnena, J.; Almgren, M. Nonradiative energy transfer in block copolymer micelles. *J. Phys. Chem.* **1991**, *95*, 4563–4568. [CrossRef]
36. Wang, Y.; Kausch, C.M.; Chun, M.; Quirk, R.P.; Mattice, W.L. Exchange of chains between micelles of labeled polystyrene-block-poly(oxyethylene) as monitored by nonradiative singlet energy transfer. *Macromolecules* **1995**, *28*, 904–911. [CrossRef]

37. Sidorov, S.N.; Bronstein, L.M.; Valetsky, P.M.; Hartmann, J.; Coelfen, H.; Schnablegger, H.; Antonietti, M. Stabilization of metal nanoparticles in aqueous medium by poly(ethylene oxide)-poly(ethylene imine) block copolymers. *J. Colloid Interface Sci.* **1999**, *212*, 197–211. [CrossRef]
38. Spatz, J.P.; Sheiko, S.; Möller, M. Ion stabilized block copolymer micelles film formation and inter micellar interaction. *Macromolecules* **1996**, *29*, 3220–3226. [CrossRef]
39. Lazzari, M.; Scalarone, D.; Hoppe, C.E.; Vazquez-Vazquez, C.; Lòpez-Quintela, M.A. Tunable polyacrylonitrile based micellar aggregates as a potential tool for the fabrication of carbon nanofibers. *Chem. Mater.* **2007**, *19*, 5818–5820. [CrossRef]
40. Qiu, L.Y.; Bae, Y.H. Polymer Architecture and Drug Delivery. *Pharm. Res.* **2006**, *23*, 1–30. [CrossRef]
41. Karanikolopoulos, N.; Pitsikalis, M.; Hadjichristidis, N.; Georgikopoulou, K.; Calogeropoulou, T.; Dunlap, J.R. pH-Responsive aggregates from double hydrophilic block copolymers carrying zwitterionic groups. Encapsulation of antiparasitic compounds for the treatment of leishmaniasis. *Langmuir* **2007**, *23*, 4214–4224. [CrossRef]
42. Kwon, G.S.; Okano, T. Polymeric micelles as new drug carriers. *Adv. Drug Deliv. Rev.* **1996**, *21*, 107–116. [CrossRef]
43. Karanikolopoulos, N.; Zamurovic, M.; Pitsikalis, M.; Hadjichristidis, N. Poly(DL-lactide)-*b*-Poly(N,N-dimethylamino-2-ethyl methacrylate): Synthesis, characterization, micellization behaviour in aqueous solutions and encapsulation of the hydrophobic drug dipyridamole. *Biomacromolecules* **2010**, *11*, 430–438. [CrossRef]
44. Li, J.; Barrow, D.; Howell, H.; Kalachandra, S. In vitro drug release study of methacrylate polymer blend system: Effect of polymer blend composition, drug loading and solubilizing surfactants on drug release. *J. Mater. Sci. Mater. Med.* **2010**, *21*, 583–588. [CrossRef]
45. Heinzmann, C.; Salz, U.; Moszner, N.; Fiore, G.L.; Weder, C. Supramolecular Cross-Links in Poly(alkyl methacrylate) Copolymers and Their Impact on the Mechanical and Reversible Adhesive Properties. *ACS Appl. Mater. Interf.* **2015**, *7*, 13395–13404. [CrossRef] [PubMed]
46. Khai, N.; Nguyen, H.; Dang, H.H.; Nguyen, L.T.; Nguyen, L.M.T.; Truong, T.T.; Nguyen, H.T.; Nguyen, T.Q.; Tran, C.D.; Nguyen, L.-T.T. Self-healing elastomers from supramolecular random copolymers of 4-vinyl pyridine. *Eur. Polym. J.* **2023**, *199*, 112474. [CrossRef]
47. Trubetskoy, V.S. Polymeric micelles as carriers of diagnostic agents. *Adv. Drug Deliv. Rev.* **1999**, *37*, 81–88. [CrossRef]
48. Gerst, M.; Schuch, H.; Urban, D. *Amphiphilic Block Copolymers as Surfactants in Emulsion Polymerization*; ACS Symposium Series; Glass, J.E., Ed.; ACS Publications: Washington, DC, USA, 2000; Volume 765, pp. 37–51.
49. Yu-Su, S.Y.; Thomas, D.R.; Alford, J.E.; LaRue, I.; Pitsikalis, M.; Hadjichristidis, N.; DeSimone, J.M.; Dobrynin, A.V.; Sheiko, S.S. Molding copolymer micelles: A framework for molding of discrete objects on surfaces. *Langmuir* **2008**, *24*, 12671–12679. [CrossRef] [PubMed]
50. Kataoka, K.; Harada, A.; Nagasaki, Y. Block copolymer micelles for drug delivery: Design, characterization and biological significance. *Adv. Drug Deliv. Rev.* **2001**, *47*, 113–131. [CrossRef] [PubMed]
51. Bronstein, L.M.; Sidorov, S.N.; Valetsky, P.M.; Hartmann, J.; Coelfen, H.; Antonietti, M. Induced micellization by interaction of poly(2-vinylpyridine)-block-poly(ethylene oxide) with metal compounds. Micelle characteristics and metal nanoparticle formation. *Langmuir* **1999**, *15*, 6256–6262. [CrossRef]
52. Munch, M.R.; Gast, A.P. Kinetics of block copolymer adsorption on dielectric surfaces from a selective solvent. *Macromolecules* **1990**, *23*, 2313–2320. [CrossRef]
53. Breulmann, M.; Förster, S.; Antonietti, M. Mesoscopic surface patterns formed by block copolymer micelles. *Macromol. Chem. Phys.* **2000**, *201*, 204–211. [CrossRef]
54. Roka, N.; Pitsikalis, M. Synthesis and micellization behavior of amphiphilic block copolymers of poly(N-vinyl pyrrolidone) and poly(benzyl methacrylate): Block versus statistical copolymers. *Polymers* **2023**, *15*, 2215. [CrossRef] [PubMed]
55. Kontoes-Georgoudakis, P.; Plachouras, N.V.; Kokkorogianni, O.; Pitsikalis, M. Amphiphilic block copolymers of poly(N-vinyl pyrrolidone) and poly (isobornyl methacrylate). Synthesis, characterization and micellization behaviour in selective solvents. *Eur. Polym. J.* **2024**, *208*, 112873. [CrossRef]
56. Roka, N.; Pitsikalis, M. Statistical copolymers of N-vinylpyrrolidone and benzyl methacrylate via RAFT: Monomer reactivity ratios, thermal properties and kinetics of thermal decomposition. *J. Macromol. Sci. Part A Pure Appl. Chem.* **2018**, *55*, 222–230. [CrossRef]
57. Karatzas, A.; Bilalis, P.; Iatrou, H.; Pitsikalis, M.; Hadjichristidis, N. Synthesis of well-defined functional macromolecular chimeras based on poly(ethylene oxide) or poly(N-vinyl pyrrolidone). *React. Funct. Polym.* **2009**, *69*, 435–440. [CrossRef]
58. Bilalis, P.; Zorba, G.; Pitsikalis, M.; Hadjichristidis, N. Synthesis of poly(n-hexyl isocyanate-b-N-vinylpyrrolidone) block copolymers by the combination of anionic and nitroxide-mediated radical polymerizations: Micellization properties in aqueous solutions. *J. Polym. Sci. Part A Polym. Chem. Ed.* **2006**, *44*, 5719–5728. [CrossRef]
59. Bilalis, P.; Pitsikalis, M.; Hadjichristidis, N. Controlled nitroxide-mediated and reversible addition-fragmentation chain transfer polymerization of N-vinylpyrrolidone: Synthesis of block copolymers with styrene and 2-vinylpyridine. *J. Polym. Sci. Part A Polym. Chem. Ed.* **2006**, *44*, 659–665. [CrossRef]

60. Roka, N.; Kokkorogianni, O.; Pitsikalis, M. Statistical copolymers of N-vinylpyrrolidone and 2-(dimethylamino)ethyl methacrylate via RAFT: Monomer reactivity ratios, thermal properties, and kinetics of thermal decomposition. *J. Polym. Sci. Polym. Chem.* **2017**, *55*, 3776–3787. [CrossRef]
61. Fokaidis-Psyllas, A.; Kokkorogianni, O.; Pitsikalis, M. Statistical copolymers of N-vinylpyrrolidone and phenoxyethyl methacrylate via RAFT polymerization: Monomer reactivity ratios, thermal properties, kinetics of thermal decomposition and self-assembly behavior in selective solvents. *Polym. Bull.* 2025; *in press*. [CrossRef]
62. Plachouras, N.V.; Pitsikalis, M. Statistical copolymers of N–vinylpyrrolidone and 2–chloroethyl vinyl ether via radical RAFT polymerization: Monomer reactivity ratios, thermal properties, and kinetics of thermal decomposition of the statistical copolymers. *Polymers* **2023**, *15*, 1970. [CrossRef]
63. Roka, N.; Papazoglou, T.P.; Pitsikalis, M. Block copolymers of Poly(N–vinylpyrrolidone) and Poly(vinyl esters) bearing n-alkyl side groups via radical RAFT polymerization: Synthesis, characterization and thermal properties. *Polymers* **2024**, *16*, 2447. [CrossRef]
64. Rinno, H. Poly(vinyl esters). In *Ullmann's Encyclopedia of Industrial Chemistry*; Wiley-VCH Verlag GmbH&Co. KGaA: Weinheim, Germany, 2000; Volume 28, pp. 469–479.
65. Murray, R.E.; Lincoln, D.M. Catalytic route to vinyl esters. *Catal. Today* **1992**, *13*, 93–102. [CrossRef]
66. Charmot, D.; Corpart, P.; Adam, H.; Zard, S.Z.; Biadatti, T.; Bouhadir, G. Controlled radical polymerization in dispersed media. *Macromol. Symp.* **2000**, *150*, 23–32. [CrossRef]
67. Matioszek, D.; Brusylovets, O.; Wilson, D.J.; Mazières, S.; Destarac, M. Reversible addition-fragmentation chain-transfer polymerization of vinyl monomers with N,N-dimethylsdiselenocarbamates. *J. Polym. Sci. Part A Polym. Chem.* **2013**, *51*, 4361–4368. [CrossRef]
68. Benard, J.; Favier, A.; Zhang, L.; Nilararoya, A.; Davis, T.P.; Barner-Kowollik, C.; Stenzel, M.H. Poly(vinyl ester) star polymers via xanthate-mediated living radical polymerization: From poly(vinyl alcohol) to glycopolymer stars. *Macromolecules* **2005**, *38*, 5475–5484. [CrossRef]
69. Gu, Y.; He, J.; Li, C.; Zhou, C.; Song, S.; Yang, Y. Block copolymerization of vinyl acetate and vinyl neo-decanoate mediated by dithionosulfide. *Macromolecules* **2010**, *43*, 4500–4510. [CrossRef]
70. Lipscomb, C.E.; Mahanthappa, M.K. Poly(vinyl ester) block copolymers synthesized by reversible addition-fragmentation chain transfer polymerizations. *Macromolecules* **2009**, *42*, 4571–4579. [CrossRef]
71. Lipscomb, C.E.; Mahanthappa, M.K. Microphase separation mode-dependent mechanical response in poly(vinyl ester)/PEO triblock copolymers. *Macromolecules* **2011**, *44*, 4401–4409. [CrossRef]
72. Zhu, P.; Liu, Y.; Yang, H.; Chen, X. Effect of non-ideal mixed solvents on dimensions of poly(N-vinylpyrrolidone) and poly(methyl methacrylate) coils. *J. Macromol. Sci. Part B Polym. Phys.* **2006**, *45*, 1125–1134.
73. Provencher, S.W. CONTIN: A general purpose constrained regularization program for inverting noisy linear algebraic and integral equations. *Comput. Phys. Commun.* **1982**, *27*, 229–242. [CrossRef]
74. Antonietti, M.; Heinz, S.; Schmidt, M.; Rosenauer, C. Determination of the Micelle Architecture of Polystyrene/Poly(4-vinylpyridine) Block Copolymers in Dilute Solution. *Macromolecules* **1994**, *27*, 3276–3281. [CrossRef]
75. Pitsikalis, M.; Hadjichristidis, N.; Mays, J.W. Model Mono-, Di-, and Tri-ω-Functionalized Three-Arm Star Polybutadienes. Association Behavior in Dilute Solution by Dynamic Light Scattering and Viscometry. *Macromolecules* **1996**, *29*, 179–184. [CrossRef]
76. Ghezzi, M.; Pescina, S.; Padula, C.; Santi, P.; Del Favero, E.; Cantù, L.; Nicoli, S. Polymeric micelles in drug delivery: An insight of the techniques for their characterization and assessment in biorelevant conditions. *J. Control. Release* **2021**, *332*, 312–336. [CrossRef] [PubMed]
77. Li, T.; Nowell, C.J.; Cipolla, D.; Rades, T.; Boyd, B.J. Direct Comparison of Standard Transmission Electron Microscopy and Cryogenic-TEM in Imaging Nanocrystals Inside Liposomes. *Mol. Pharm.* **2019**, *16*, 1775–1781. [CrossRef]

Disclaimer/Publisher's Note: The statements, opinions and data contained in all publications are solely those of the individual author(s) and contributor(s) and not of MDPI and/or the editor(s). MDPI and/or the editor(s) disclaim responsibility for any injury to people or property resulting from any ideas, methods, instructions or products referred to in the content.